17th Australasian Fluid Mechanics Conference
Auckland, New Zealand
5-9 December 2010

# Two-point Correlation Statistics in the Atmospheric Surface Layer

**K. Chauhan, N. Hutchins, J. Monty and I. Marusic**

Department of Mechanical Engineering
The University of Melbourne, Parkville, Victoria 3010, Australia

## Abstract

A collaborative experimental effort in the western Utah salt flats [7] has enabled us to map coherence in turbulent boundary layers at very high Reynolds numbers [$Re_\tau \approx O(10^6)$]. It is found that the large-scale coherence recently noted in the logarithmic region of laboratory-scale boundary layers [4] is also present in the very high Reynolds number atmospheric surface layer [5]. Two-point correlation for the streamwise fluctuation is compared for the stable, neutral and unstable surface layers in a plane parallel to the surface. The observed differences in the spatial features of the correlation maps can be characterized by the stability parameter $z/\zeta$. Further, the integral length scales obtained from the correlation show orderly behavior with varying stability.

## Introduction

In the past few decades, significant research has been dedicated to identifying and studying coherence in canonical wall bounded turbulent flows. In boundary layer flows, the presence of hairpin packets/structures is well-accepted [2, 3]. Hutchins & Marusic [4] have shown the presence of large meandering features in the overlap region of the boundary layer, associating its presence to be consistent with hairpin formations and evidenced its signature in the two-point correlation. The two-point correlation in atmospheric surface layers have been studied by number of researchers for LES studies [1, 8, 9]. Further, Marusic & Hutchins [9], Marusic & Heuer [8] and Hutchins *et al.* [5] have revealed the similarity of two-point correlation statistics between laboratory and atmospheric flows. The structure of neutral surface layer over the western Utah salt flats at the Surface Layer Turbulence and Environmental Science Test Facility (SLTEST) was the focus of these studies [7]. Hutchins *et al.* [5] provided affirmation of large scale coherence in the neutral surface layer that is similar to observations made in very high Reynolds number laboratory scale boundary layers. Our present study focuses on similar statistics for the atmospheric surface layer where thermal buoyancy effects are present (both positive and negative). The available literature on stable and unstable surface layer flows has primarily focussed on second-order turbulence and single-point correlation statistics; e.g., Monin-Obukhov (M-O) similarity [6, 10]. In this paper we examine the similarities and differences in the two-point correlation of the streamwise fluctuations in the plane parallel to the surface between stable, neutral and unstable surface layers.

The measurements were acquired by a spanwise and wall-normal array of sonic anemometer (Campbell Scientific CSAT3) in an 'L' shaped configuration at the SLTEST facility. The spanwise array was placed over an overall distance of 27m with 10 anemometers placed 3m apart and at a height of $z$ =2.14m. The schematic of this arrangement is shown in figure 1. Here only the results of two-point correlations from the spanwise array are presented. Capitalized velocities (e.g. $U$) and overbars indicate time-averaged values; lowercase notation (e.g. $u$) denote fluctuating components. Further details of the experimental setup can be found in [5].

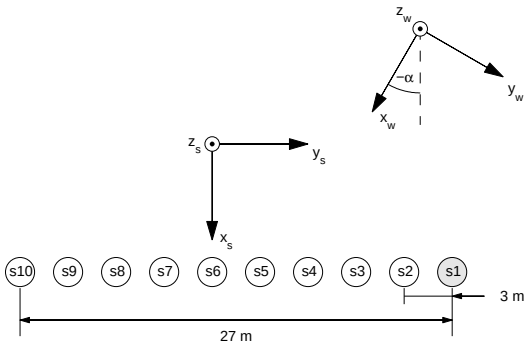


Figure 1: Plan view sketch of the sonic anemometer array.

As the surface layer is influenced by the diurnal cycle of heating and cooling, the temperature at the surface is elevated resulting in increased heat flux $\overline{w\theta}$ during the daytime. The measurements were acquired over a period of nine days over which the unstable flow conditions primarily existed. At night, long periods of near zero heat flux were recorded, and the surface layer is analogous to a canonical turbulent boundary layer (neutral). Suitable stable conditions also existed making it feasible to compare these three broad categories of surface layer flows over a flat terrain.

The stability of the boundary layer is characterized by the Monin-Obukhov stability parameter $z/\zeta$, where $\zeta$ is the Obukhov length.

$$\frac{1}{\zeta} = -\frac{\kappa g\,(\overline{w\theta})_0}{\overline{\theta}\,u_*^3}. \tag{1}$$

Here, $\kappa = 0.41$ is the von Kármán constant, $g$ is the gravitational acceleration, $u_* = (-\overline{uw})_0^{1/2}$ is the scaling velocity obtained at $z$ =2.14m, $(\overline{w\theta})_0$ is the surface heat flux, and $\overline{\theta}$ is the mean temperature. The statistics are examined over an hour of data that was sampled at 20 Hz. The data were pre-processed to obtain velocities in the mean wind direction (principal velocity component along $x_w$ in figure 1) and filtered to remove large scale weather related variations (de-trending). A total of 74 hours of data from the nine days were found to be suitable for analysis; i.e., absence of large flow angles relative to the sonic axis ($x_s$ in figure 1), absence of large variations in flow velocity and temperature and positive velocity relative to the sonic axis. Taylor's hypothesis is used to convert from time to space in the streamwise direction ($x$); i.e., $\Delta x = U\Delta t$, where the convection velocity $U$ is the mean velocity.

## Results

Figure 2 shows a two-point correlation map of streamwise velocity fluctuations $R_{uu}$ (equation 2) in the $x$-$y$ (streamwise/spanwise) plane obtained using the spanwise array of sonic anemometers for the neutral surface layer.

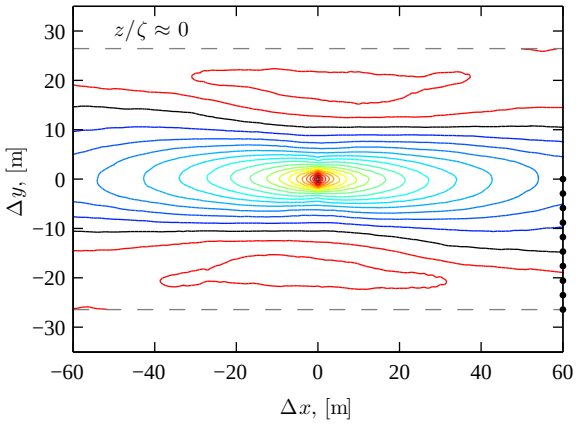


Figure 2: Iso-contours of two-point correlation of streamwise fluctuations $R_{uu}$ in the streamwise/spanwise plane for the neutral surface layer. The contour levels are shown in increments of 0.05. Black contour line denotes $R_{uu} = 0$. Dashed grey line indicates the maximum spanwise extent of correlation map that can be obtained using the 10 sonic anemometers indicated by the black bullet marks.

$$R_{uu}(\Delta x, \Delta y) = \frac{\overline{u(x+\Delta x, y+\Delta y, z)u(x, y, z)}}{\sigma_u^2} \qquad (2)$$

The stability parameter for this flow condition is nearly zero and the measurement was obtained between 04:00 to 05:00 on 2 June 2005. The same hour of data is used by Hutchins *et al.* [4, 5] to show similarity of the neutral surface layer to laboratory flow. Based on the similarity of neutral surface layer with the zero pressure gradient laboratory flow, Hutchins *et al.* also estimated the surface layer thickness ($\delta$) for this flow condition to be approximately 60m. However, it is not feasible to determine $\delta$ for the stable and unstable surface layer. In our objective to compare the *relative* changes in the structure of two-point correlations we therefore keep the abscissae and ordinates dimensional in figures 2, 3 and 4.

For the neutral case in figure 2, the region of positive $R_{uu}$ correlation is highly elongated in the streamwise direction. Considering the surface layer thickness $\delta \approx 60$m [5], this region of positive correlation has a much larger extent than the conventional wisdom about large turbulent scales (of the order of $\delta$). It is also seen that the positive $R_{uu}$ is accompanied by a region of negative $R_{uu}$ on either side in the spanwise direction, although the magnitude is not high. Statistically this suggests that a low-speed $u$ event at $\Delta x = 0$ and $\Delta y = 0$ is most likely to be accompanied by low speed fluid surrounding it, while high speed fluid is likely to be found at farther $\Delta y$ in the spanwise direction at the same time. Hutchins *et al.* [4, 5] have evidenced such low speed streaks by showing instantaneous velocity fields that exhibit presence of long meandering low velocity flow regimes that span almost $10\delta$ in the streamwise direction. This suggests that large scale turbulence features present in the surface layer can approach the kilometer scale.

The two point correlation $R_{uu}$ for the stable and unstable surface layer from an hour of measurement is mapped in figures 3 and 4, respectively. On first observation it can be readily noticed that the correlation map alters significantly under the buoyant conditions. An elongated region of positive $R_{uu}$ in the stable surface layer still exists; however, its streamwise and spanwise extent are significantly reduced. The correlation quickly drops to near zero in both the streamwise and spanwise directions indicating

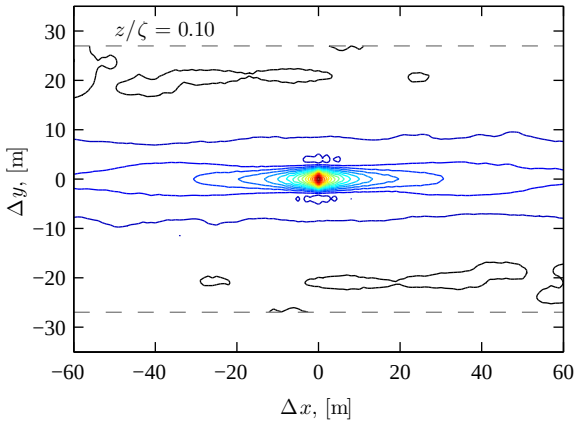


Figure 3: Iso-contours of $R_{uu}$ for the stable surface layer. See figure 2 for details.

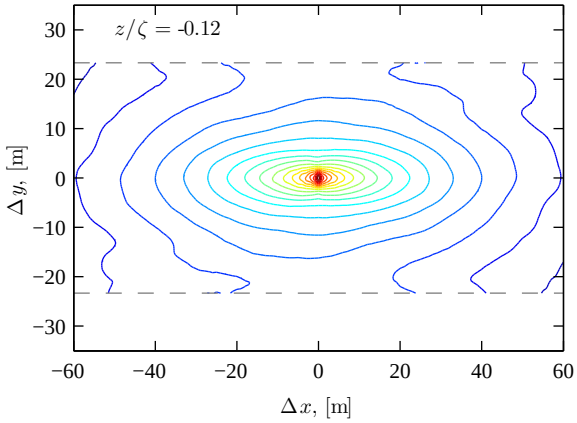


Figure 4: Iso-contours of $R_{uu}$ for the unstable surface layer. See figure 2 for details

that any coherence in the turbulence has a relatively short spatial reach. The change in $R_{uu}$ map for the unstable surface layer relative to the neutral case is in the opposite sense compared to the stable surface layer. It is seen that the correlation is higher overall. Unlike the neutral case we do not see any negative correlation at higher $\Delta y$, although we are limited by the physical extent of our measurement array in mapping $R_{uu}$ at farther $\Delta y$. Regardless, it can be said that the unstable surface layer likely shows similar evidence of low/high speed flow regimes (around the condition point at $\Delta x = 0$ and $\Delta y = 0$) with a much larger spatial extent than the neutral case.

For an unstable surface layer the heat flux is positive, which results in buoyancy assisted turbulence production along with that from the shear. Increased temperature fluctuations due to the strong thermal gradient couple with wall-normal fluctuations which indirectly also increase the $\overline{uw}$, the Reynolds stress component responsible for majority of turbulence production due to shear. The increased turbulence manifests itself into the footprint of the $R_{uu}$ maps as seen earlier, indicative of large scale coherence. For the stable surface layer, the thermal gradient is negative and it acts to suppress the temperature fluctuations. Further, density stratification also contributes to attenuation of wall-normal fluctuations which inhibit mechanisms of wall-turbulence. Hence for the stable surface layer we find that turbulence becomes weak and lacks large scale coherence.

To characterize the changes in spatial attributes of the correla-

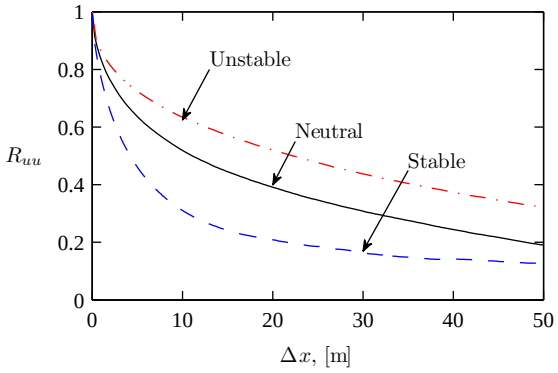


Figure 5: Two-point correlation of the streamwise fluctuations $R_{uu}$ in the streamwise direction. Black '——': Neutral, $z/\zeta \approx 0$; blue '– – –': stable, $z/\zeta \approx 0.1$; and red '– · – · –': unstable, $z/\zeta \approx -0.1$.

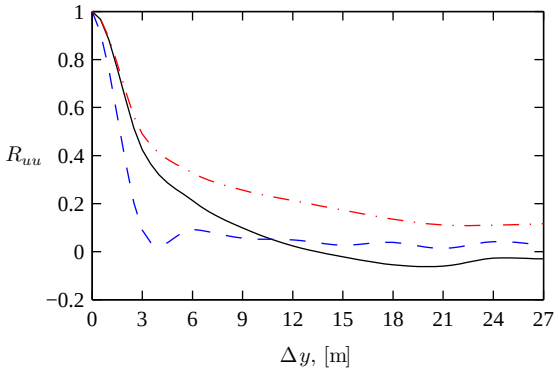


Figure 6: Two-point correlation of the streamwise fluctuations $R_{uu}$ in the spanwise direction. Black '——': Neutral, $z/\zeta \approx 0$; blue '– – –': stable, $z/\zeta \approx 0.1$; and red '– · – · –': unstable, $z/\zeta \approx -0.1$.

tion map we compare the integral length scales that can be determined from two-point correlation. Figure 5 shows line plots of $R_{uu}$ versus the lead/lag in the streamwise direction for the stable, neutral and unstable cases. The values of $R_{uu}$ shown in figure 5 can be traced from the contour levels along $\Delta y = 0$ in figures 2, 3 and 4. The observations made earlier from the correlation maps are now distinctively clear from the line plots. The decrease in $R_{uu}$ is the steepest for the stable surface layer while strong correlation exists for large lead/lag for the unstable case. One can now integrate under these curves to obtain a representative streamwise integral length scale for the streamwise fluctuations. We integrate $R_{uu}$ until it remains positive after its initial descent from $R_{uu} = 1$ to obtain the integral length scale as,

$$\Lambda_x = \int_0^{x(R_{uu}>0)} R_{uu}(r, \Delta y = 0)\, \mathrm{d}r\,. \tag{3}$$

Similarly, figure 6 shows the line plots of $R_{uu}$ versus the lead/lag in the spanwise direction. The values of $R_{uu}$ in figure 6 can be traced from the contour levels along $\Delta x = 0$ in figures 2, 3 and 4. Again observations that are consistent with the correlation map can be made regarding variation of $R_{uu}$ with $\Delta y$. For the neutral surface layer, distinct positive and negative region exists while $R_{uu}$ for the unstable case is positive throughout the width of the measurement array (27m). In this case, it is not possible to

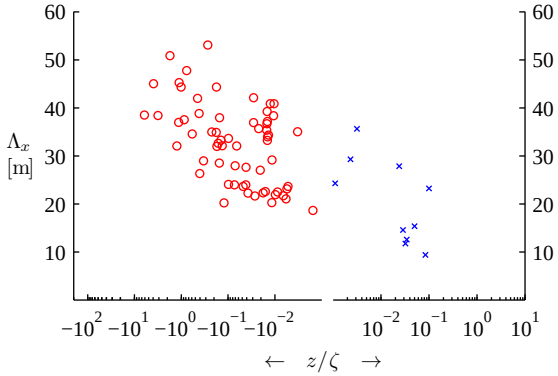


Figure 7: Variation of streamwise integral length scale $\Lambda_x$ with stability parameter $z/\zeta$ for the streamwise fluctuations obtained from the spanwise array at $z = 2.14$m. Red '$\circ$' denote unstable ($z/\zeta < 0$) surface layer data. Blue '$\times$' denote stable ($z/\zeta > 0$) surface layer data. Note that both positive and negative abscissae are on logarithmic scale.

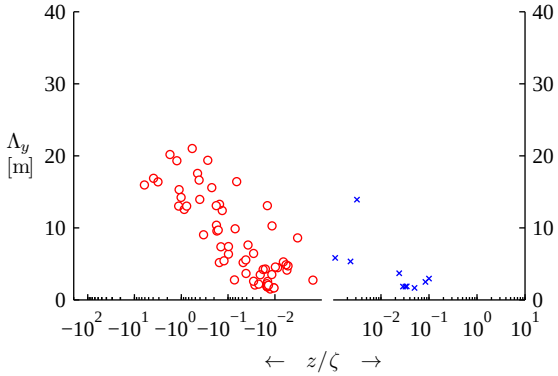


Figure 8: Variation of spanwise integral length scale $\Lambda_y$ with stability parameter $z/\zeta$. See figure 7 for details.

obtain the zero crossing of $R_{uu}$ in the spanwise direction. With an emphasis only on examining the relative differences between the neutral, stable and unstable surface layer we integrate $R_{uu}$ up to the available $\Delta y = 27$m in the spanwise direction to obtain the spanwise integral length scale for streamwise fluctuations as,

$$\Lambda_y = \int_0^{y=27\mathrm{m}} R_{uu}(\Delta x = 0, r)\, \mathrm{d}r\,. \tag{4}$$

Results from equations 3 and 4 are shown in figures 7 and 8, respectively. The integral scales are plotted versus the stability parameter $z/\zeta$. It is found that both integral length scales show an overall increasing trend with decreasing stability (increasing $-z/\zeta$). The trend is also seen for the stable surface layers; however, in the present dataset we do not have enough hourly stable flow conditions to establish the certainty of its trend. Overall, the unstable surface layer data indicates that the integral scale changes with a logarithmic trend with a changing stability parameter. Although it should be noted that such logarithmic trends cannot exist for both stable and unstable cases without a discontinuity for neutral surface layers ($z/\zeta = 0$). Further, it should be appreciated that the integral scales in the atmospheric surface layers can be very large, $O(100\mathrm{m})$, while the same in a typical laboratory boundary layer would be only few centimeters.

## Conclusions

We have compared the two-point correlation in the $x$-$y$ plane to identify systematic differences in the structure of $R_{uu}$ between the stable, neutral and unstable surface layers. The surface heat flux is the key mechanism that imposes the differences observed. The increased turbulence under positive surface heat flux results in an increased spatial extent of correlation levels of significant magnitude. Extending the comparison made by Hutchins *et al.* [5] we can say that similar large scale features and associated wall-mechanisms also occur in the unstable surface layer at a larger physical scale. The difference in the structure of $R_{uu}$ is characterized by the stability parameter $z/\zeta$ by evaluating the integral length scales in the streamwise and spanwise directions. Both $\Lambda_x$ and $\Lambda_y$ show consistent trends that appear to be logarithmic with varying stability. The ability to estimate the integral lengths scale characterized by $z/\zeta$ can be incorporated in near-wall models of large-eddy simulations of atmospheric flows. Finally, the present results represent surface layer flows where the stability variations are not too severe away from the neutral conditions. That is, most hourly flow conditions follow the Monin-Obukhov similarity. Hence caution is recommended when interpreting these results for stable and unstable surface layers that do not adhere to M-O similarity.

## References


[1] Carper, M. A. and Porté-Agel, F., The role of coherent structures in subfilter-scale dissipation of turbulence measured in the atmospheric surface layer, *J. Turb.*, **5**, 2004, N 40.

[2] Christensen, K. T. and Adrian, R. J., Statistical evidence of hairpin vortex packets in wall turbulence, *J. Fluid Mech.*, **431**, 2001, 433–443.

[3] Ganapathisubramani, B., Hutchins, N., Hambleton, W. T., Longmire, E. K. and Marusic, I., Investigation of large-scale coherence in a turbulent boundary layer using two-point correlations, *J. Fluid Mech.*, **524**, 2005, 57–80.

[4] Hutchins, N. and Marusic, I., Evidence of very long meandering streamwise structures in the logarithmic region of turbulent boundary layers, *J. Fluid Mech.*, **579**, 2007, 1–28.

[5] Hutchins, N., Marusic, I. and Klewicki, J., Atmospheric scale streakiness: Evidence of very large-scale coherent structures in high Reynolds number atmospheric turbulent boundary layers, *Boundary-Layer Meteor.*, Under review.

[6] Kaimal, J. C. and Finnigan, J. J., *Atmospheric Boundary Layer Flows: Their Structure and Measurement*, Oxford University Press, New York, 1994.

[7] Klewicki, J. C., Foss, J. F. and Wallace, J. M., High Reynolds number [$R_\theta$=O($10^6$)] boundary layer turbulence in the atmospheric surface layer above western Utah's salt flats, in *Flow at Ultra-High Reynolds and Rayleigh Numbers*, editors R. J. Donnelly and K. R. Sreenivasan, Springer, 1998, 450–466.

[8] Marusic, I. and Heuer, W., Reynolds number invariance of the structure inclination angle in wall turbulence, *Phys. Rev. Lett.*, **99**.

[9] Marusic, I. and Huthcins, N., Study of the log-layer structure in wall turbulence over a very large range of Reynolds number, *Flow Turb. Combus.*, **81**, 2008, 115–130.

[10] Pahlow, M., Parlange, M. and Porté-Agel, F., On Monin-Obukhov similarity in the stable atmospheric boundary layer, *Boundary-Layer Meteor.*, **99**, 2001, 225–248.